Published in final edited form as:
Int J Radiat Oncol Biol Phys. 2007 October 1; 69(2): 381–389.

Patterns of Recurrence Analysis in newly diagnosed GBM following 3D Conformal Radiation Therapy with respect to Pre-RT MR Spectroscopic Findings

Ilwoo Park, BS[1,2], **Gregory Tamai, BS**[1], **Michael C. Lee, Ph.D.**[1], **Cynthia F. Chuang, Ph.D.**[3], **Susan M. Chang, M.D.**[4], **Mitchel S. Berger, M.D.**[4], **Sarah J. Nelson, Ph.D.**[1,2], and **Andrea Pirzkall, M.D.**[1,3,4]

1*Surbeck Laboratory of Advanced Imaging, Department of Radiology, University of California, San Francisco, CA*

2*UCSF/UCB Joint Graduate Group in Bioengineering, University of California, San Francisco, CA*

3*Department of Radiation Oncology, University of California, San Francisco, CA*

4*Department of Neurological Surgery, University of California, San Francisco, CA*

Abstract

Purpose—To determine whether the combined MRI and MR spectroscopy imaging (MRSI) prior to radiation therapy (RT) is valuable for RT target definition, and to evaluate the feasibility of replacing the current definition of uniform margins by custom shaped margins based on the information from MRI and MRSI.

Methods and Materials—Twenty three GBM patients underwent MRI and MRSI within 4 weeks after surgery but before the initiation of RT and at two month follow-up (FU) intervals thereafter. MRSI data were quantified on the basis of a Choline-to-NAA Index (CNI) as a measure of spectroscopic abnormality. A combined anatomic and metabolic ROI (MRI/S) consisting of T2-weighted hyperintensity, contrast enhancement (CE), resection cavity and CNI2 based on the pre-RT imaging was compared to CNI2 extent and RT dose distribution. The spatial relationship of the pre-RT MRI/S and the RT dose volume was compared to the extent of CE at each FU.

Results—Nine patients showed new or increased CE during FU, and 14 patients were either stable or had decreased CE. New or increased areas of CE occurred within CNI2 that was covered by 60 Gy in six patients and within the CNI2 that was not entirely covered by 60 Gy in three patients. New or increased CE resided within the pre-RT MRI/S lesion in 89 % (8/9) of the patients with new or increased CE.

Conclusion—These data indicate that the definition of RT target volumes according to the combined morphologic and metabolic abnormality may be sufficient for RT targeting.

Address correspondence to: Andrea Pirzkall, M.D., Center for Molecular and Functional Imaging, 185 Berry Street, Suite 350, Box 0946, San Francisco, CA 94107-1739, *Email*: apirzkall@radonc.ucsf.edu, *Phone*: (415) 353-9405, *Fax*: (415) 353-9425.

Conflicts of Interest Any actual or potential conflicts of interest do not exist for publishing this article. This work has not been submitted for publication elsewhere.

Keywords

Magnetic resonance spectroscopy imaging; Brain Tumor; GBM; Conformal radiation therapy; Pattern of recurrence

INTRODUCTION

High-grade malignant gliomas are the most common primary brain tumors in adults. Despite recent developments in surgical techniques and postoperative treatment, the prognosis for patients with a high-grade glioma remains very poor. The median survival has been reported in the range of 12 – 15 months for patients with glioblastoma multiforme (GBM) and 36 months for anaplastic astrocytoma (AA) [1–4]. Conventional treatment of high-grade gliomas includes surgical resection which provides immediate decompression and yields tissue for histopathologic evaluation. This is typically followed by concurrent radiation/chemotherapy.

In order to enhance the effectiveness of radiation therapy (RT) in gliomas while sparing normal tissue, it is important to accurately distinguish cancer from normal tissue. Computerized tomography (CT) and magnetic resonance imaging (MRI) are currently used to delineate the target volume for high grade gliomas with MRI providing superior soft tissue contrast [5–7]. Target volumes for 3D conformal radiation therapy (3D-CRT) are defined to cover the Gadolinium contrast enhancing region on T1-weighted images obtained from MRI with a uniform margin of 1 to 4 cm [1,8–10] and/or the area of hyperintense lesion on T2-weighted MRI enlarged by several centimeters [11,12].

These uniform margins are defined in an attempt to address several shortcomings with conventional anatomic imaging. Serial biopsy studies show tumor cells more than 3 cm from the contrast enhancing (CE) region [13]; in addition, some tumors are not contrast-enhancing, and the T2 hyperintensity (T2h) may not distinguish tumor from edema, or normal appearing brain tissue beyond T2h might harbor tumor cells. Previous studies have shown that three-dimensional (3D) magnetic resonance spectroscopic imaging (MRSI) is valuable for mapping the spatial extent of brain tumors and this technique is suggested as an adjunct to MRI in delineating the target for radiation therapy in high-grade gliomas (HGG) [14,15].

Three-dimensional proton MR spectroscopy imaging (MRSI) provides information concerning the spatial distribution of cellular metabolites in the brain. At long echo times (TE 144ms), it provides information about levels of metabolites such as choline (Cho), creatine (Cr), N-acetyl-aspartate (NAA), and lipid/lactate (LL). NAA is a neuronal marker that is decreased in tumors. Creatine provides a measure of cellular bioenergetic processes, and may be a marker for cell oxygenation. Cho is a membrane component that is increased in tumors due to increased proliferation and/or increased membrane turnover. Lactate and lipid are presumed to represent measures of hypoxia and necrosis, respectively.

A series of image-guided biopsies have been performed at our institution in an attempt to study the biological significance of these imaging parameters. Dowling et al. correlated metabolite levels measured by preoperative MRSI with histologic findings from image-guided biopsies of brain tumors [16]. The findings showed that when the pattern of MRS metabolites included abnormally increased Cho and decreased NAA resonances, the histology of such biopsy samples invariably confirmed the presence of tumor. This prompted the development of an automated analysis that estimates peak parameters for Choline and NAA on a voxel-by-voxel basis (including normal appearing brain tissue) and computes the so-called Cho-to-NAA Index (CNI). A CNI of 2 or greater has been shown to correspond to tumor in biopsy correlation studies [17,18].

In previous studies, we have compared the differences between MRSI and MRI lesions in patients with HGG. We found significant variations between the two modalities with respect to tumor size and location prior to surgery [14], and after surgery but before RT [15]. These data suggested that MRSI is likely to improve the diagnostic accuracy of the assessment of residual disease for HGG. It was concluded that the incorporation of metabolic information into the treatment planning of postoperative HGG patients would result in target volumes different in size and shape compared to the currently defined target volumes as described above.

The purpose of this study is to determine whether the combination of MRI and MRSI is of value for RT target definition. In particular, we sought to assess the feasibility of replacing the current definition of uniform margins by custom shaped margins in accordance to the tumor extent seen on MRI and MRSI in order to limit RT exposure to normal brain tissue. We therefore compared the spatial location and extent of CE at follow-up imaging with the actually delivered radiation dose and related those to spectroscopic findings prior to RT in order to assess the potential for modifying the RT target volume.

METHODS AND MATERIALS

A total of thirty adult patients (22M/8F; median age 57 years, range 27–80 years) with WHO II classified glioblastoma multiforme (GBM) who were treated at the University of California, San Francisco, Medical Center between March 2000 and October 2004 were recruited for this retrospective study. Each patient underwent MRI and MRSI within 4 weeks after surgery but before RT (pre-RT). Follow-up (FU) exams with MRI/MRSI were acquired at the end of RT and at two month intervals thereafter. To be included in this study, patients must have had a pre-RT MRI and MRSI and at least one FU that included post contrast imaging. Another requirement was the availability of the radiation treatment plan. Seven patients were excluded due to incomplete follow-up data (4), an alignment failure between the pre-RT and the FU exams (1), lack of spectroscopy at pre-RT (1), or a lack of availability of the radiation treatment plan (1), leaving a total of 23 patients for evaluation.

The median age of the 23 patients studied was 53 years at the pre-RT time point with a range of 27 – 76 years. The Karnofsky performance scale (KPS) was ≥ 70. Written and informed consent for participating in the study was obtained from all patients. All 23 patients were treated with fractionated 3D-CRT and chemotherapy whereby three patients received more than one chemotherapeutic agent. Chemotherapeutic agents included Temozolomide (13), Thalidomide (3), Poly ICLC (6), Zarnestra (1), Tarceva (1), Accutane (1) and Celebrex (1), and 2 patients underwent carbogen breathing during delivery of RT following injection of bovine hemoglobin (HbOC-201). Chemotherapy was given either concurrently (15) or adjuvantly (8).

Radiation target volumes were defined based on current standard of care without knowledge of the MRSI data. The conventional target volume was defined to encompass the region of hyperintensity on T2-weighted MR images with a uniform margin of about 1 cm and/or the region of contrast enhancement plus a margin of 2–3 cm. The addition of the 1–3 cm margin to the target volume was designed to account for microscopic tumor infiltration. The latter target volume was reduced after delivery of about 46 Gy (so called cone down) in about half of the patients and an additional 14 Gy was prescribed to the region of contrast enhancement plus a margin of about 1–2 cm. A total dose of 60 Gy was delivered in 30 fractions over a course of approximately 6 weeks by means of an average of 3 to 5 non-coplanar treatment portals designed to achieve at least 95% target coverage while meeting surrounding structure dose constraints.

MRI/MRSI Acquisition

Patients were scanned on a 1.5 T GE Signa MR scanner (GE Healthcare, Milwaukee, WI) using a quadrature head coil. The MRI protocol included an axial T2-weighted fluid attenuated inversion recovery (FLAIR) sequence [19,20] with 3-mm slice thickness and pre- and post-Gadolinium-DTPA T1-weighted spoiled gradient echo (SPGR) images with 1.5-mm thickness. At the end of the MRI scan, 3D MRSI was acquired using Point Resolved Spectroscopic (PRESS) [21] volume localization with spectral spatial pulses for water suppression and very selective suppression (VSS) pulses for outer volume suppression (TR/TE=1000/144 ms, 1 cc nominal spatial resolution; 12×12×8 or 16×8×8 phase-encoding matrix) [22]. Spectral values were normalized relative to the noise standard deviation, estimated from the right hand end of the spectra which was devoid of metabolite peaks [23]. The MRSI data were quantified offline to estimate peak parameters for the metabolites within the excited region. A Choline-to-NAA Index of greater than 2 (CNI2) was calculated automatically and respective contours of CNI2 were displayed on the anatomic images. The details of the acquisition parameters of the MRI and MRSI examinations and the spectral processing have been published elsewhere [23,24, 25].

MRI and MRSI data were aligned to the post contrast T1-weighted images. The treatment planning CT and the actually delivered RT dose distribution were obtained and registered to the latter in order to correlate the radiation dose distribution with the MRI and MRSI data [26–28].

ROIs and MRI/MRSI volumetric evaluation

The MRI data sets were contoured manually and verified by a radiation oncologist (AP). Regions of interest (ROI) included contrast enhancement (CE) on T1-weighted post contrast images and the hyperintensity on T2-weighted images (T2h), and the resection cavity (RC, the latter because it is included in the conventional RT target definition). Any regions of intrinsic T1 shortening, i.e. blood, were accounted for based on the pre-contrast T1-weighted images and subtracted from the CE ROI. The CNI2 contour was automatically generated by a previously described automated image analysis program [17]. Because of current size and shape limitations, the PRESS volume did not always cover ROIs in their entire extent, we restricted our subsequent data analysis to the portion of these lesions that were within the PRESS volume.

The overall morphologic abnormality, which serves for the standard RT target volume definition, was defined as CE + T2h + RC (Figure 1a). The addition of the metabolic abnormality (CNI2) to the morphologic abnormality defined the combined volume of MRI/S.

The radiation treatment plans that were actually delivered to the patients were retrieved from the department of radiation oncology at UCSF and the delivered isodose lines were uploaded into our image analysis programs. The MRI/S volume and the perpendicular distance of its maximum extension beyond the 60 Gy isodose line (60 Gy) were calculated. The volume and the maximum extension of CNI2 outside the 60 Gy were also calculated in order to evaluate whether the entire region of the metabolic abnormality as defined by CNI2 was covered by the current conventional target definition and dose distribution.

The follow-up imaging data sets were aligned to the pre-RT reference T1-weigheted post contrast SPGR data set [29]. Post-RT areas of CE (as a conventional measure of possible tumor recurrence) were contoured and the pre-RT ROI's including PRESS, CNI2, 60 Gy, and the combined volume of MRI/S were superimposed and compared to the post-RT CE for analysis (Figure 1b). The volume and the maximum extension of CE at each follow-up scan beyond the pre-RT MRI/S were calculated. The spatial correspondence of CE during follow-up and the

pre-RT CNI2 were analyzed to evaluate the degree of new/increased CE residing within or beyond CNI2 and to see whether this area of CNI2 was covered by 60 Gy. In addition, the total volumes of CE as well as the volume of CE within the PRESS volume were evaluated.

Changes in CE volume during FU were classified as “increased” (>25% increase in CE volume), “new” (onset of new CE in patients without CE residual disease at pre-RT), “stable” (less than 25% +/− volume change), or “decreased” (>25% decrease in CE volume). Upon declared clinical progression (in light of new or increased CE and neurological or neurocognitive symptoms), patients were enrolled into different treatment protocols and at that point excluded from this current analysis.

RESULTS

Pre-RT

Prior to RT, 21 of 23 patients showed contrast enhancing lesions with a median CE volume of 10.1 cc, ranging from 0.4 to 42.0 cc. The median CE volume covered by the PRESS volume was 6.3 cc, and ranged from 0.2 to 35.5 cc. The median CE volume outside the PRESS volume was 1.9 cc, and ranged from 0.05 to 11.8 cc.

There were portions of the MRI/S abnormality (CNI2+CE+T2h+RC) that were not covered by the prescribed dose of 60 Gy in 11/23 patients. Among these 11 patients, 10 showed regions of CNI2 that were not covered by 60 Gy. The median volume of CNI2 that extended beyond the prescribed dose volume was 3.5 cc (range: 0.2 – 29.2 cc), and it extended as much as 4 cm from the 60 Gy isodose contour (median 1.7, range: 0.4 – 4.0 cm). Five of the 10 patients had only minor extensions of CNI2 which were less than 2 cc. Table 1 summarizes the pre-RT results.

Figure 2 shows an example of one of the 10 patients who had CNI2 extensions suggestive of tumor infiltration along the posterior genu of the corpus callosum that was not covered by 60 Gy. The dose display for this patient shows that the majority of the CNI2 which extended beyond the 60 Gy region received ≥50 Gy, with a small portion of CNI2 receiving 40 Gy. The actually delivered doses in such CNI2 extension areas varied across these 10 patients. Five of them received between 50 and 60 Gy to the CNI2 region outside 60 Gy, one patient received between 40 and 60 Gy, and four patients received between 30 and 60 Gy.

The volume of “normal” brain tissue within the spectroscopically evaluated region that was morphologically intact and exhibited normal metabolite levels that was exposed to the prescribed dose of 60 Gy exhibited a rather large median volume of 78.5 cc (range 20.1– 135.9 cc) compared to the volume of MRI/S (median 38.8, range 10.6 – 107.9 cc) (Table 2).

Post-RT follow-up with respect to the RT dose

The changes in CE were evaluated with respect to the pre-RT parameters in all 23 patients during follow-up examinations (Table 3). The CE volume inside PRESS was calculated at each FU scan, and compared to that of the pre-RT scan. Median FU for all patients was 6 months with a range of 1.7 to 16.5 months. Three of the 23 patients showed stable CE, 11 showed decreasing CE (Figure 3b). A total of 9 patients showed new or increased CE on their FU scans that resided within the pre-RT CNI2 (Figure 3a). Six of them showed CE within the CNI2 that was covered by 60 Gy (see example in Figure 4), and 3 of them showed CE within the CNI2 that was not entirely covered by 60 Gy (see example in Figure 5). The first of those three patients (pt 1 in Figure 3a) progressed through the course of RT and developed a large contrast enhancing cyst with considerable midline shift 2 months after the start of RT. This patient deceased shortly thereafter. The second patient (pt 2 in Figure 3a) showed new CE inferior to the resection cavity, as well as enlarged CE around the resection cavity 10 months after RT.

The volume of CE extending outside of the 60 Gy volume was 3 cc. This patient responded initially to RT with an overall decrease in CE volume, but showed a significant increase in CE volume at 10 months follow-up. The third patient (pt 3 in Figure 3a) showed increased CE volume around the resection cavity at 8 months after RT, and the volume of CE extending beyond the 60 Gy volume was 3.7 cc.

Post-RT Follow-up with respect to MRI/S

We assessed whether the addition of MRS to conventional MRI target definition would have predicted regions of new or increasing CE at follow-up. For each follow-up scan, we evaluated the extent of new or increased CE and compared it at the time of progression to the size of the pre-RT MRI/S volume. Three patients showed increasing CE at the 2 month FU whereby the new or increased CE resided within the combined MRI and MRSI abnormality (MRI/S) as assessed at pre-RT in 2 of 3 patients (Table 4). Increased CE was found to extend beyond the pre-RT MRI/S at the 2 month FU exam in the one patient described above who developed a significant tissue shift due to the formation of a large contrast enhancing cyst (Figure 6). The patient deceased shortly thereafter. At 4 months post RT, new or increased CE was observed in 2 patients confined to the pre-RT MRI/S. At 6 months, 2 patients showed new or increased CE. One of them showed new or increased CE residing within the MRI/S region. The other patient had showed some increase (<25%) in his CE pattern at his prior FU but increased further at 6 months and exceeded by then beyond the pre-RT MRI/S. This can be interpreted as the result of continued outgrowth from the initial recurrence pattern which was originally confined within the MRI/S lesion, as opposed to a recurrence that originated outside the combined MRI/S volume at pre-RT. One patient at 8 months and another at 10 months after RT showed new or increased CE whereby the new or increased CE was found confined within the pre-RT MRI/S volume.

Relationship between volumes receiving 60 Gy and MRI/S lesions

For the 9 patients with new or increased CE, the median 60 Gy volume was 126.9 cc (range 81.2 – 163.9 cc), which is significantly larger than the volume of MRI/S (median 47.2 cc; range 15.3 – 80.2 cc), thereby leaving a large portion of normal brain tissue that received 60 Gy (Table 2). Figure 7 shows 2 examples in which the volume of 60 Gy is compared to the volume of MRI/S. Figure 7a depicts an example case where the 60 Gy isodose contour largely surrounds the volume of MRI/S leaving a considerable portion of morphologically and metabolically normal appearing brain tissue arguably over treated with 60 Gy. Defining the target volume based on the combined metabolic and morphologic information could have spared a substantial volume of brain tissue irradiated. Figure 7b shows another example case in which the difference between the volumes of 60 Gy and MRI/S was minimal, but the 60 Gy isodose contour failed to cover the entire MRI/S abnormal region because the target definition was based on the MRI abnormality alone.

DISCUSSION

We have retrospectively evaluated whether a new approach for RT target definition that adds MR based information on metabolic abnormality (CNI2) to the conventional RT target definition is likely to be sufficient in defining the possible regions of new or increasing CE that develop following conventional 3D conformal RT.

The conventional target definition and dose prescription for RT as applied in the herein evaluated GBM patients status post surgical resection was found to cover the majority of MRSI metabolic disease. However, the prescribed dose of 60 Gy did not cover all pre-RT tumor extensions with tumor suggestive metabolic activity in 48% (11/23) of the patients (Table 1). This CNI2 extension ranged in volume and was rather small in most cases but extended as

much as 4 cm beyond the 60 Gy isodose line and was found to be covered by RT doses of at least 30 Gy. Based on our recurrence analysis with respect to the pre-RT MRI/S volume, we believe that this CNI2 extension outside the 60 Gy volume is not the initial focus of tumor recurrence, but we observed that CE seemed to expand, i.e. the tumor grew into these regions during FU.

All recurrence patterns analyzed in this study were local, and no distant failures were observed. These findings are consistent with prior studies that have shown that the vast majority of recurrences occur within 2 cm of the original tumor site [10,30,31] or “in field” (more than 80% of the tumor recurrence residing within the prescription isodose) [32]. The results summarized in Table 3 show that the increased CE, as a presumed sign of tumor recurrence, occurred both within and beyond the prescribed dose of 60 Gy. Increased CE was found within the region of the CNI2 that extended beyond the 60 Gy isodose line in three patients. As pointed out above, tumor seems to be growing into these regions rather than originating from there. In other words, tumor growth or recurrence as demarcated by breakdown of the blood-brain barrier is confined to the metabolically active tumor regions as assessed prior to RT. It is not expected that the inclusion of the CNI2 volume into the 60 Gy volume would improve tumor control but spare normal tissue.

The MRI/S volume may be considered as a new way to define custom shaped target volumes which seems to contain the recurrence effectively within the first year of RT. We have shown that 89 % of the patients exhibited recurrence patterns contained within the pre-RT MRI/S volume (Table 4). This suggests that if we had reshaped the target definition using the MRI/S volume, we could have reduced the irradiated volume to morphologically and metabolically normal brain tissue, but still covered the recurrent tumor. Whether this approach would result in the same pattern of recurrence still remains to be assessed in a clinical trial. In particular, it remains to be shown that reducing tumor margins would not result in worsened tumor control if one assumes that the herein described lack of recurrence in normal appearing brain may be related to the efficacy of RT.

Our findings have importance for the target definition of high-grade gliomas and low-grade gliomas alike [33]. Conventionally employed large uniform margins have been historically utilized due to the inability to demarcate “invisible” tumor extent. They typically expose a rather large volume of normal appearing brain arguably unnecessary. The new approach of custom shaped margins in accordance to metabolic and morphologic abnormality will allow for the sparing of normal tissue as well as reducing the overall volume of tissue radiated, and thereby reduce side effects. This will allow the exploitation of focal therapies including delivery if high focal doses to tumor subregions that deem radioresistant or particularly aggressive, i.e. high proliferative potential. Such regions can be demarcated by MRSI and/or other metabolic imaging techniques either prior to RT or at the end of RT by means of assessing a serial response pattern. Studies in this regard are currently ongoing.

Adverse side effects following brain irradiation and the resulting compromised clinical outcome can be minimized by limiting the volume of irradiated brain tissue. Such central nervous system side effects include impaired intellectual function and hypothalamic-pituitary dysfunction. The risk of radiation necrosis is rather unlikely following a conventional dose of 60 Gy delivered in standard fractionation of 2 Gy/30 fractions but rises rapidly as the radiation dose increases above 60 Gy [34].

We found for the herein evaluated patient population that the volume of brain tissue that was treated with 60 Gy but appeared morphologically and metabolically normal was rather large, nearly double the median volume of the MRI/S. With respect to local control, all patients’ recurrence seemed to originate within the combined MRI/S abnormality except for one patient

with debatable outcome due to significant tissue shift (Fig. 6). This suggests that tissue sparing seems feasible using modern RT coupled with customized target definition that is based upon the combined morphologic/metabolic imaging.

Current technical limitations in regard to the size and shape of the PRESS region prescribed for MRS evaluation are likely to be overcome shortly with the design of more effective suppression pulses that will allow the size of the selective volume to be adjusted to different head sizes and shapes, allowing the spectroscopic analysis of larger regions of supratentorial brain tissue.

CONCLUSIONS

Increased CE during FU was observed to occur within the combined MRI/S volume as defined at pre-RT in all but one patient, for whom a large cyst caused a significant tissue shift. This suggests that the definition of RT target volumes according to the morphologic and metabolic abnormality (MRI/S) may be sufficient for RT targeting. MRSI in combination with MRI may thus allow for a reduction and custom shaping of currently employed target volumes for RT in brain gliomas which would reduce the dose exposure to uninvolved normal brain tissue.

Acknowledgment

This work has been presented in part at the 13th Annual meeting of ISMRM, Miami, Florida 2005

The research was supported by grants: SPORE P50 CA97297 and RO1 CA-59-880, National Institutes of Health/ National Cancer Institute, Washington D.C.

REFERENCES

1. Bleehen NM, Stenning SP. A Medical Research Council trial of two radiotherapy doses in the treatment of grades 3 and 4 astrocytoma. The Medical Research Council Brain Tumour Working Party. Br J Cancer 1991;64:769–774. [PubMed: 1654987]
2. Leibel SA, Scott CB, Loeffler JS. Contemporary approaches to the treatment of malignant gliomas with radiation therapy. Semin Oncol 1994;21:198–219. [PubMed: 8153665]
3. Walker MD, Strike TA, Sheline GE. An analysis of dose-effect relationship in the radiotherapy of malignant gliomas. Int J Radiat Oncol Biol Phys 1979;5:1725–1731. [PubMed: 231022]
4. Stupp R, Mason WP, van den Bent MJ, et al. Radiotherapy plus concomitant and adjuvant temozolomide for glioblastoma. N Engl J Med 2005;352:987–996. [PubMed: 15758009]
5. Ten Haken RK, Thornton AF Jr, Sandler HM, et al. A quantitative assessment of the addition of MRI to CT-based, 3-D treatment planning of brain tumors. Radiother Oncol 1992;25:121–133. [PubMed: 1332134]
6. van Kampen M, Levegrün S, Wannenmacher M. Target volume definition in radiation therapy. Br J Radiol 1997;70:S25–S31. [PubMed: 9534715]
7. Sheline GE. Radiotherapy for high grade gliomas. Int J Radiat Oncol Biol Phys 1990;18:793–803. [PubMed: 2182578]
8. Garden AS, Maor MH, Yung WK, et al. Outcome and patterns of failure following limited-volume irradiation for malignant astrocytomas. Radiother Oncol 1991;20:99–110. [PubMed: 1851573]
9. Liang BC, Thornton AF Jr, Sandler HM, et al. Malignant astrocytomas: focal tumor recurrence after focal external beam radiation therapy. J Neurosurg 1991;75:559–563. [PubMed: 1653309]
10. Wallner KE, Galicich JH, Krol G, et al. Patterns of failure following treatment for glioblastoma multiforme and anaplastic astrocytoma. Int J Radiat Oncol Biol Phys 1989;16:1405–1409. [PubMed: 2542195]
11. Nakagawa K, Aoki Y, Fujimaki T, et al. High-dose conformal radiotherapy influenced the pattern of failure but did not improve survival in glioblastoma multiforme. Int J Radiat Oncol Biol Phys 1998;40 (5):1141–1149. [PubMed: 9539570]

12. Fitzek MM, Thornton AF, Rabinov JD, et al. Accelerated fractionated proton/photon irradiation to 90 cobalt gray equivalent for glioblastoma multiforme: results of a phase II prospective trial. J Neurosurg 1999;91(2):251–260. [PubMed: 10433313]
13. Kelly PJ, Daumasduport C, Kispert DB, et al. Imaging-based stereotaxic serial biopsies in untreated intracranial glial neoplasms. J Neurosurg 1987;66(6):865–874. [PubMed: 3033172]
14. Pirzkall A, Tracy MR, Edward GE, et al. MR-spectroscopy guided target delineation for high-grade gliomas. Int J Radiat Oncol Biol Phys 2001;50(4):915–928. [PubMed: 11429219]
15. Pirzkall A, Li X, Oh J, et al. 3D MRSI for resected high-grade gliomas before RT: tumor extent according to metabolic activity in relation to MRI. Int J Radiat Oncol Biol Phys 2004;59(1):126–137. [PubMed: 15093908]
16. Dowling C, Bollen AW, Noworolski SM, et al. Preoperative proton MR spectroscopic imaging of brain tumors: correlation with histopathologic analysis of resection specimens. AJNR Am J Neuroradiol 2001;22(4):604–612. [PubMed: 11290466]
17. McKnight TR, Noworolski SM, Vigneron DB, et al. An automated technique for the quantitative assessment of 3D-MRSI data from patients with glioma. J Magn Reson Imaging 2001;13(2):167–177. [PubMed: 11169821]
18. McKnight TR, von dem Bussche MH, Vigneron DB, et al. Histopathological validation of a three-dimensional magnetic resonance spectroscopy index as a predictor of tumor presence. J Neurosurg 2002;97(4):794–802. [PubMed: 12405365]
19. Rydberg JN, Hammond CA, Grimm RC, et al. Initial clinical experience in MR imaging of the brain with a fast fluid-attenuated inversion-recovery pulse sequence. Radiology 1994;193(1):173–180. [PubMed: 8090888]
20. De Coene B, Hajnal JV, Gatehouse P, et al. MR of the brain using fluid-attenuated inversion recovery (FLAIR) pulse sequences. AJNR Am J Neuroradiol 1992;13(6):1555–1564. [PubMed: 1332459]
21. Bottomley PA. Spatial localization in NMR spectroscopy in vivo. Ann N Y Acad Sci 1987;508:333–348. [PubMed: 3326459]
22. Tran TKC, Vigneron DB, Sailasuta N, et al. Very selective suppression pulses for clinical MRSI studies of brain and prostate cancer. Magn Reson Med 2000;43(1):23–33. [PubMed: 10642728]
23. Nelson SJ. Analysis of volume MRI and MR spectroscopic imaging data for the evaluation of patients with brain tumors. Magn Reson Med 2001;46(2):228–239. [PubMed: 11477625]
24. Kurhanewicz J, Vigneron DB, Nelson SJ. Three-dimensional magnetic resonance spectroscopic imaging of brain and prostate cancer. Neoplasia 2000;2(1–2):166–189. [PubMed: 10933075]
25. Nelson SJ. Multivoxel magnetic resonance spectroscopy of brain tumors. Mol Cancer Ther 2003;2(5):497–507. [PubMed: 12748312]
26. Pelizzari CA, Chen GTY, Spelbring DR, et al. Accurate 3-dimensional registration of CT, PET, and or MR images of the brain. J Comput Assist Tomogr 1989;13(1):20–26. [PubMed: 2492038]
27. Wang C, Pahl JJ, Hogue RE. A method for co-registering three-dimensional multimodality brain images. Comput Methods Programs Biomed 1994;44(2):131–140. [PubMed: 7988116]
28. Woods RP, Mazziotta JC, Cherry SR. MRI-PET registration with automated algorithm. J Comput Assist Tomogr 1993;17(4):536–546. [PubMed: 8331222]
29. Nelson SJ, Nalbandian AB, Proctor E, et al. Registration of images from sequential MR studies of the brain. J Magn Reson Imaging 1994;4(6):877–883. [PubMed: 7865950]
30. Hochberg FH, Pruitt A. Assumptions in the radiotherapy of glioblastoma. Neurology 1980;30(9):907–911. [PubMed: 6252514]
31. Oppitz U, Maessen D, Zunterer H, et al. 3D-recurrence-patterns of glioblastomas after CT-planned postoperative irradiation. Radiother Oncol 1999;53(1):53–57. [PubMed: 10624854]
32. Lee SW, Fraass BA, Marsh LH, et al. Patterns of failure following high-dose 3-D conformal radiotherapy for high-grade astrocytomas: a quantitative dosimetric study. Int J Radiat Oncol Biol Phys 1999;43(1):79–88. [PubMed: 9989517]
33. Pirzkall A, Nelson SJ, McKnight TR, et al. Metabolic imaging of low-grade gliomas with three-dimensional magnetic resonance spectroscopy. Int J Radiat Oncol Biol Phys 2002;53(5):1254–1264. [PubMed: 12128127]

34. Larson DA, Wara WM. Radiotherapy of primary malignant brain tumors. Semin Surg Oncol 1998;14 (1):34–42. [PubMed: 9407629]

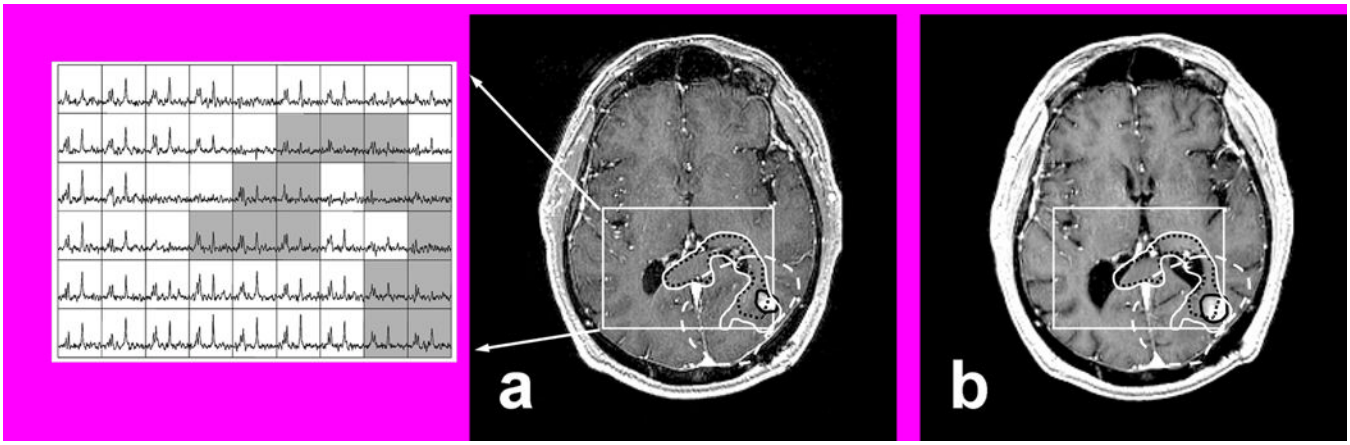

Figure 1.

T1 SPGR post contrast at pre-RT with corresponding multi-voxel spectra (a) and at 2 months post RT (b) with superimposed regions of interest (ROIs). ROIs include PRESS (rectangular box), CE (black solid line), 60 Gy (white dashed line), CNI2 (black dotted line), MRI/S (white solid line). Note that the CNI2 suggests tumor infiltration along the posterior aspect of the corpus callosum with crossing to the contralateral side which did not appear hyperintense on T2 weighted MRI.

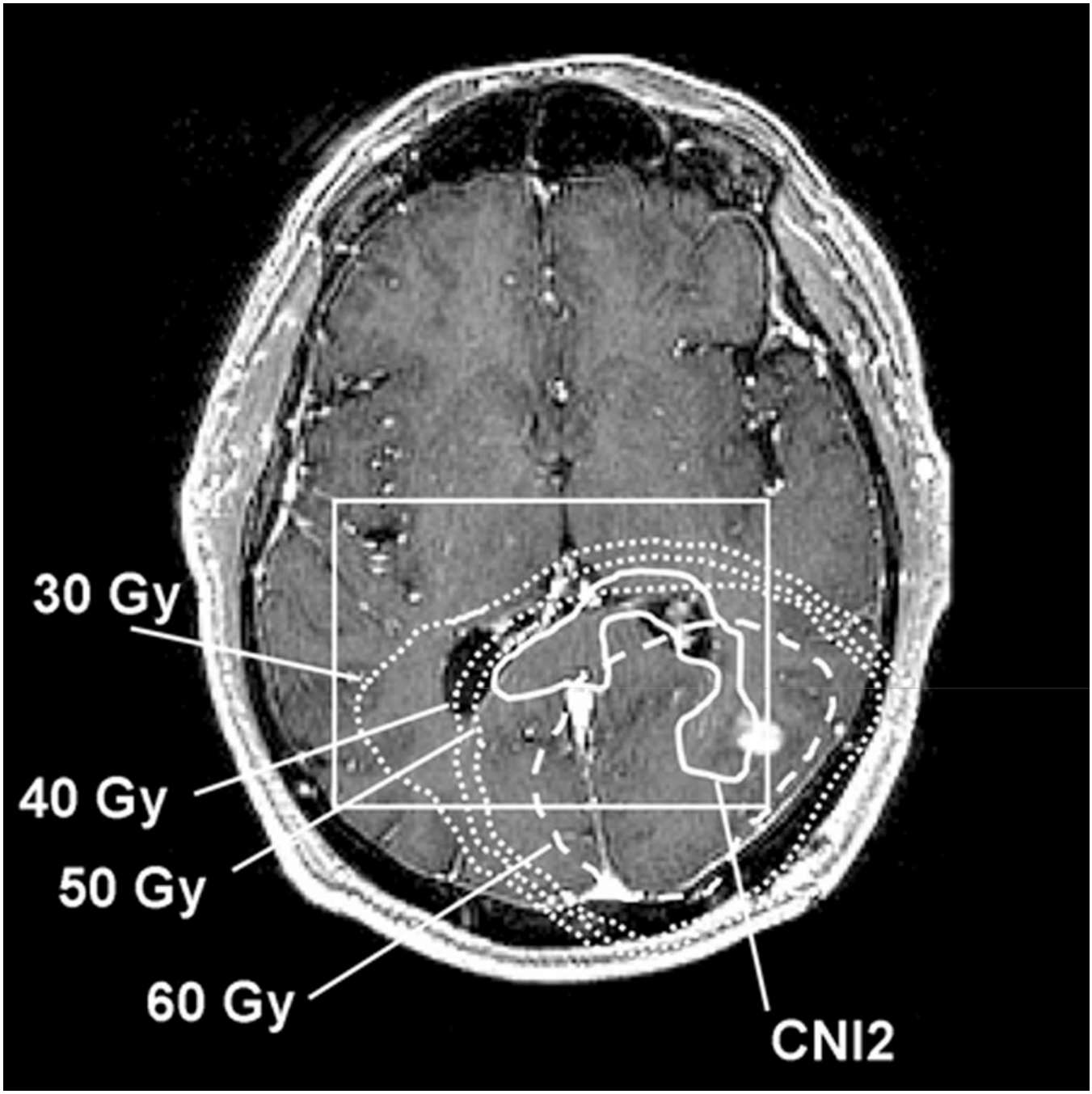

Figure 2.
Detailed dose distribution of the same patient as in Fig. 1 with the CNI2 region extending outside the 60 Gy isodose line (CNI2 solid line, 60 Gy dashed line). Additional isodose lines for 30, 40, and 50 Gy are displayed as square dotted lines (outside to inside).

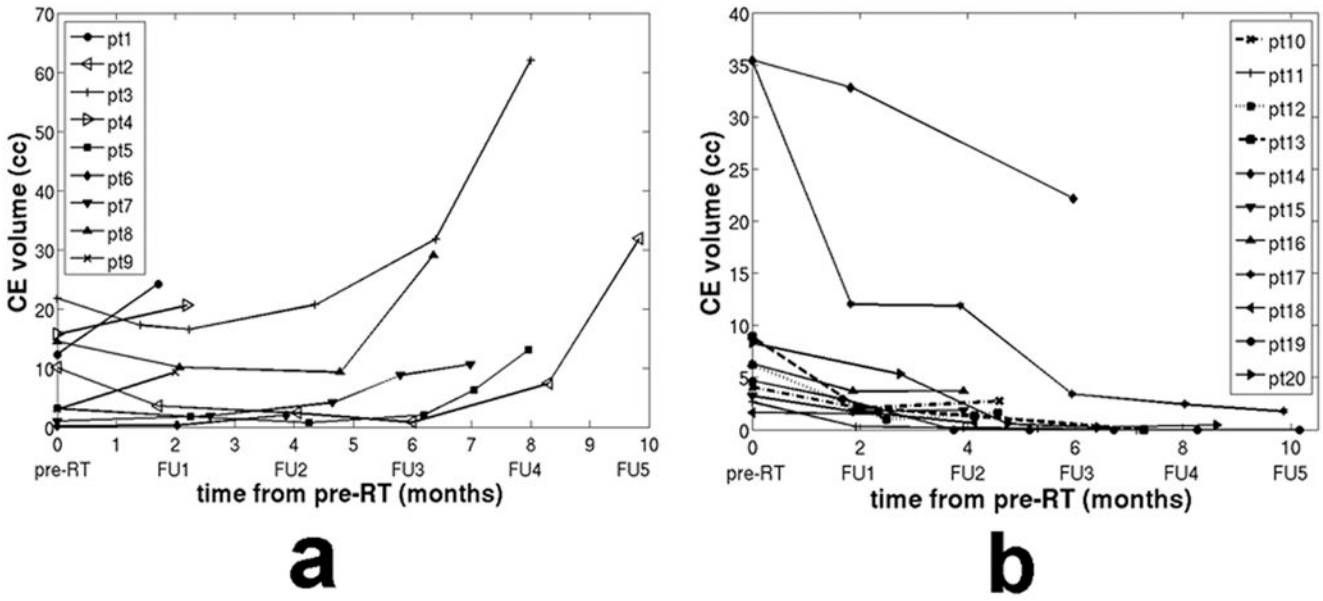

Figure 3.
CE volume change in follow-up scans for patients with a) new or increased CE, and b) decreased CE.

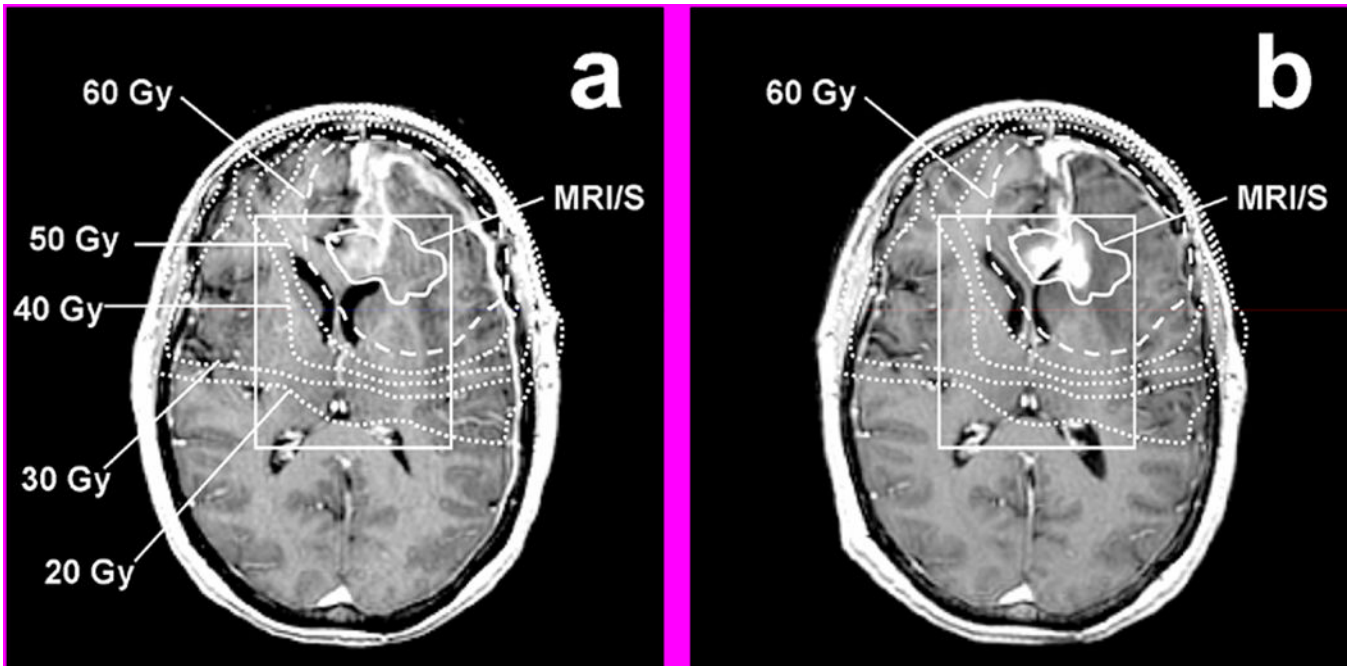

Figure 4.
Example of increasing CE within MRI/S (solid line) that was covered by 60 Gy (dashed line): (a) T1 SPGR at Pre-RT, (b) T1 SPGR at 7 months post RT

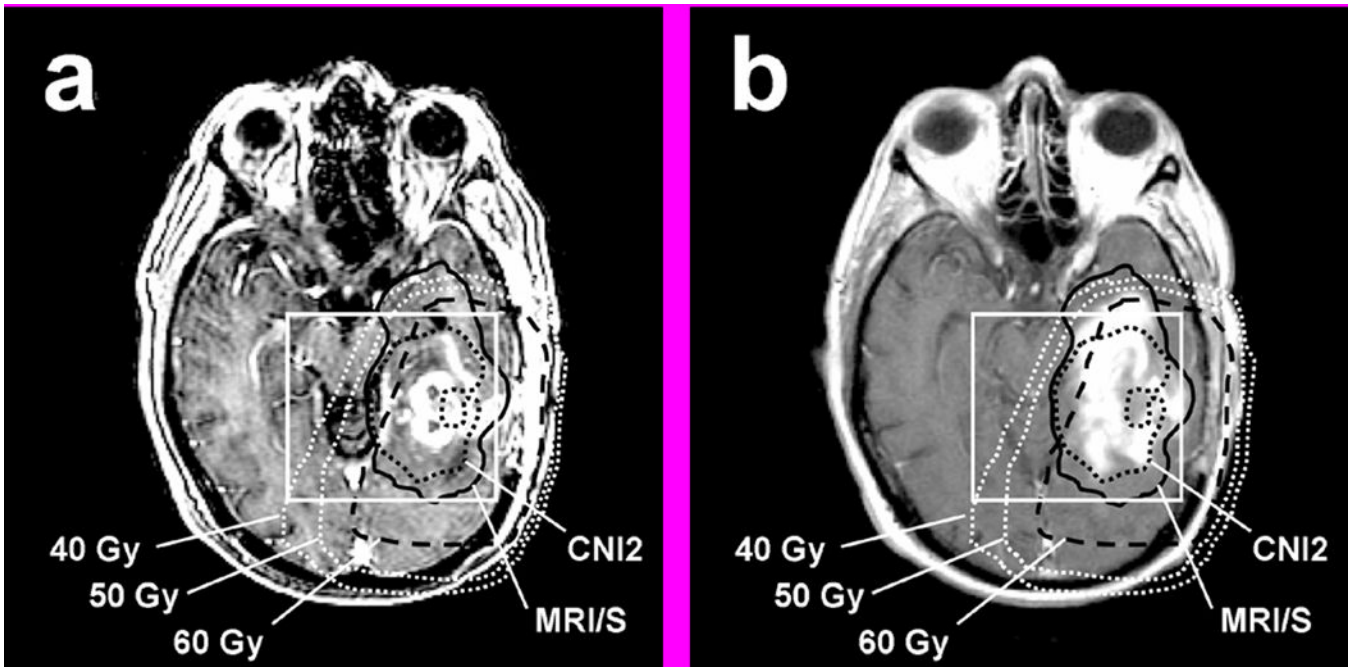

Figure 5.
Example of increasing CE within MRI/S (black solid line) that was not entirely covered by 60 Gy (black dashed line): (a) T1 SPGR at Pre-RT. (b) T1 SPGR at 8 months post RT. Note the limited coverage of the anterior and lateral portion of the temporal lobe due to current spatial and size limitations in the PRESS prescription.

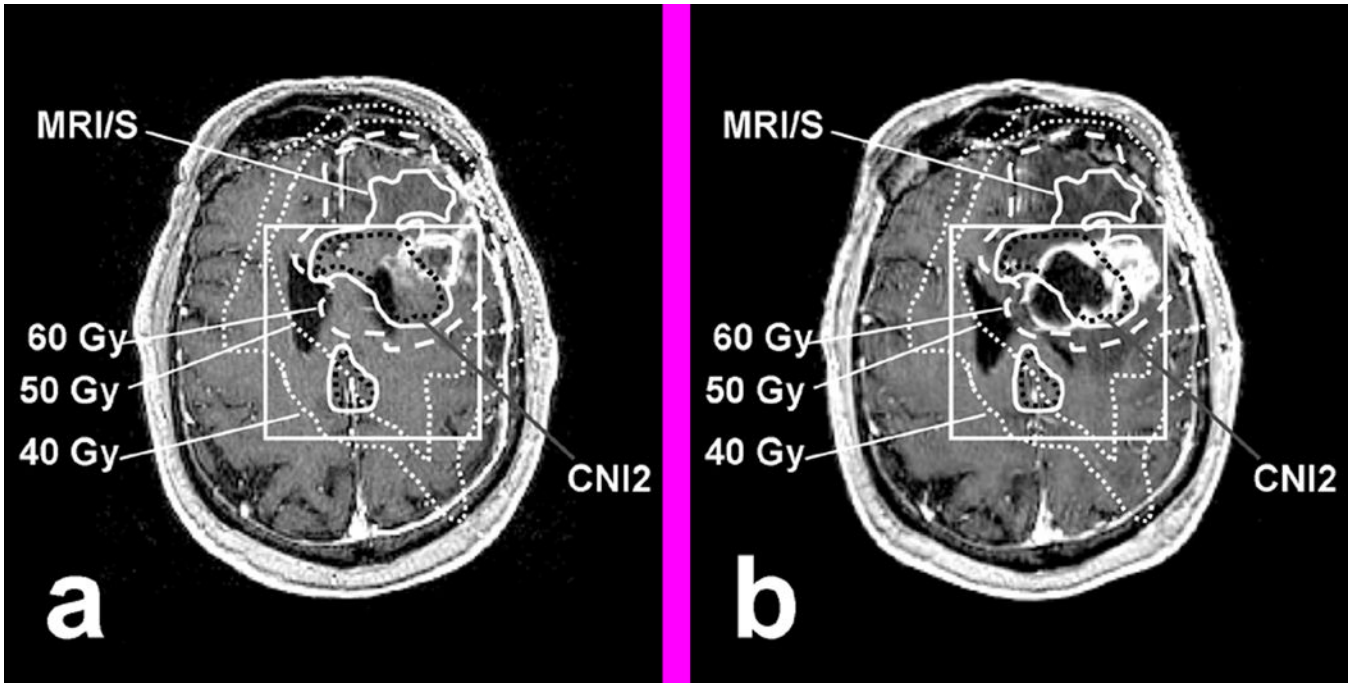

Figure 6.
The only patient in whom increased CE occurred beyond the pre-RT combined MRI/MRSI was due to the formation of a large necrotic cyst that caused a significant tissue shift: (a) T1 SPGR at Pre-RT. (b) T1 SPGR at 2 months post RT

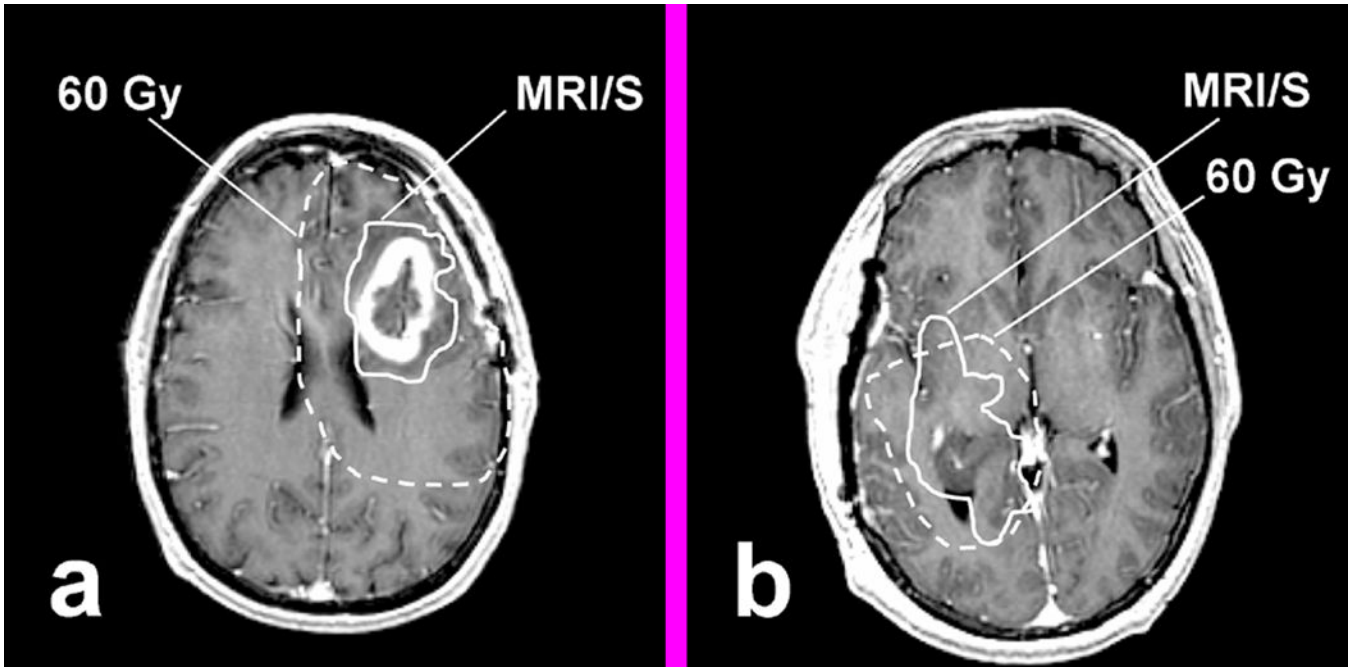

Figure 7.
Examples comparing the volume of MRI/S (solid line) and the actually delivered 60 Gy (dashed line). (a) shows typical volume of 60 Gy compared to MRI/S, which had large portion of normal appearing brain tissue that received 60 Gy, and (b) shows the case where MRI/S extended beyond 60 Gy.

Table 1

Summary of the pre-RT metabolic (CNI2) and combined modality (MRI/S) findings with respect to the actually delivered RT dose of 60 Gy.

	Number of patients	Extension volume (cc) Within PRESS [median, range]	Maximum distance (cm) [median, range]
MRI/S outside 60 Gy	11/23	5.4 (1.3 – 48.5)	2.5 (1.0 – 13.6)
CNI2 outside 60 Gy	10/23	3.5 (0.2 – 29.2)	1.7 (0.4 – 4.0)

Table 2

Volume comparison between MRI/S, normal brain tissue receiving 60 Gy, and the total volume of 60 Gy for all patients and for the subset of patients with new or increased CE. Note that the overall volume of 60 Gy was much larger than the MRI/S volume, leaving a large portion of normal brain tissue that received 60 Gy.

Number of patients	MRI/S volume (cc) [median, range]	Normal brain tissue receiving 60 Gy (cc) [median, range]	Total volume of 60 Gy (cc) [median, range]
Total 23	38.8 (10.6 – 107.9)	78.5 (20.1 – 135.9)	126.8 (71 – 165.7)
9 with new/increased CE	47.2 (15.3 – 80.2)	77.5 (44.5 – 115.5)	126.9 (81.2 – 163.9)

Table 3

Overall contrast enhancing (CE) changes in all 23 patients during follow-up (FU) relative to pre-RT

CE during FU		# patients
New/Increased CE	CE occurring within CNI2 that was ***not*** entirely covered by 60 Gy	3
	CE occurring within CNI2 that was covered by 60 Gy	6
Decreasing CE		11
Stable CE		3

Table 4

Patients with new or increased contrast enhancement (CE) during follow-up (FU), and the median volume of new or increased CE which extends beyond the volume of MRI/S.. One of the two patients at 6 months showed increased CE of >25% at 6 month FU relative to pre-RT whereby the increased CE beyond MRI/S occurred as an outgrowth from prior discernible CE changes (<25% at prior FU).

Time after RT (months)	Number of patients with new or increased CE	Number of patients with new or increased CE beyond MRI/S	Median volume of new or increased CE beyond MRI/S (cc)
2	3	1	5.1
4	2	0	-
6	2	(1)	(3.3)
8	1	0	-
10	1	0	-